

# Robot Control by Using Intelligent Systems Considering Complete Constraints

Louiza Dehyadegari<sup>1\*</sup> & Somayeh Khajehasani<sup>2</sup>

Received 28 June 2020; Revised 27 September 2020; Accepted 20 October 2020;  
© Iran University of Science and Technology 2021

## ABSTRACT

*In this paper, a multivariable control of a two-link robot is performed by fuzzy-sliding mode control. Robots on the one hand have complex dynamics due to nonlinearity, uncertainty and indeterminacy resulting from friction and other factors. The uncertainty and nonlinearity of the governing equations more and more necessitates the use of these two types of controllers in spite of a two-link and multivariable dynamic system. In this paper simulation, a fuzzy system is used in two parts. In the first part, a fuzzy system is used to approximate the uncertainty of the robot arm dynamic model in the control law and in the second part the nonlinear term of the signal function is replaced by an adaptive neuro-fuzzy controller to produce appropriate  $k$  s and to track the output properly. The comparison of simulation results suggests that the intelligent method based on the proposed adaptive neuro-fuzzy control has better performance in tracking reference signal with slight tracking error and higher accuracy compared to sliding mode method.*

**KEYWORDS:** *Two-link robot; Track of robot arm angles; Robot arm angles derivatives; Neuro-fuzzy controller; Sliding mode controller; Multivariable control.*

## 1. Introduction

Today, most of the robots are used in factories to manufacture products such as automobiles, electronic systems and also underwater or other planets explorations and with technological and robotics development, robots are used in surgeries, as nurse and relief robot, in biomechanics and nanorobotics, as replacements for body organs etc. Robots have complex dynamics due to nonlinearity, uncertainty and inflexibility in the joints. The most important obstacle in neuromuscular stimulation systems is the nonlinearity and variations of the stimulated muscle properties, muscular fatigue and daily changes in muscle properties [1]. A complete dynamic model is required in the automatic machines in the industries to control the robot arm output that is the angle of the joints. This model should provide not only the arm systematic motions but also the dynamic issues

such as the forces and torques required for these motions. Different methods like Lagrange, Newton-Euler, etc., each of which has its own advantages and disadvantages, can be used to derive the dynamic equations of mechanical systems [2].

In recent years, robotic control regarding its limitations has been considered by many researchers. Many methods (the use of neuro-fuzzy network, multi-input-multi-output adaptive control based on artificial neural networks, random search methods to find control parameters) are taken into account to design controllers and apply torque to robot [3,4]. In addition, PID controllers along with other control methods have been used to stabilize robot parameters. For instance, PID fuzzy method has been used to detect robot motion by PID controller to compensate for the turbulences and friction along the path [5]. Regarding the constraints in the input signal, in recent years some controllers have been used in which the torque applied to the mobile robot is limited and does not exceed its high bandwidth and the robot can be used to control an ideal path by these controllers [6]. The direct application of Newton's laws of motion to the simple systems

\* Corresponding author: *Louiza Dehyadegari*  
*l.dehyadegari@sirjantech.ac.ir*

1. Assistant professor Sirjan University of Technology, Sirjan, Iran.  
2. Instructor Sirjan University of Technology, Sirjan, Iran  
.Najafshahr ave. Sirjan university of technology.

motion is easy, but if the number of system particles increases, the application of laws will be difficult. In this case, Lagrange method is used. For this purpose, various control methods are used in two linear and nonlinear formats in terms of conditions. In many applications, a robot needs to move in a quiet place to perform its duty properly, therefore with this in mind it should be noted that which path is taken by robot to perform its duty that in addition to its safety, its goal can be achieved at the lowest cost. One of the suggested methods to solve this problem is planning algorithms. A method called planning quick search was proposed by Lavelle in 1998 [7]. Additionally, many methods including potential field fuzzy logic-based approach [8] and random search methods have been proposed that are among the most important methods in random path planning and lead to easier identification of control parameters but the estimation method used in these control methods does not have high accuracy.

However, the update on the degree of bias towards the target and the unexplored environments at each stage has led to the creation of appropriate methods in different environments [9]. In the researches done by Philip Chen et al (2014) a summary of adaptive neural networks is studied. In this method, the adaptive control system is examined in a multi-input-multi-output nonlinear network based on neural network. In this paper a combination of neural networks and

fuzzy logic will be used as adaptive neuro-fuzzy networks for better robot system tracking and exposure to systemic uncertainties [10,11].

The second part of the article is allocated to two-degree- of- freedom arm modeling. Two-degree-of-freedom dynamic model is obtained by the Lagrangian method. From the control point of view, these robots need particular control methods due to complex dynamics, uncertainty and unstable modes. The proposed method in the second part is a combination of neural networks and fuzzy logic that is suggested as adaptive neuro-fuzzy networks. The third part focuses on simulation results. In short, the purpose of these simulations and studies is to finally achieve a control method with high efficiency and accuracy despite the existing constraints on the angles and angular velocity of these robots. In the end, we will have conclusion and suggestions for further research.

## 2. The Introduction of Two-Degree-of-Freedom Robot Arm and Its Modeling

In this chapter, the dynamic modeling of robot arm is written by Lagrange equation. According to the model obtained, a combination of neural and fuzzy networks will be used in both output tracking and uncertainties approximation in order to control the two-link robot arm that its block diagram is shown in Fig.1.

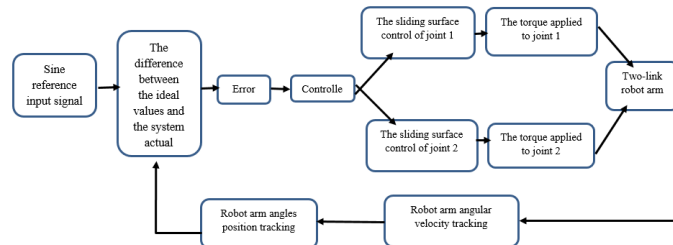


Fig. 1. The robot arm controller block diagram in terms of sine reference input signal

### 2.1. The kinematics

The kinematics describes robot motion regardless of the forces and torques creating them. Kinematics is a geometric description [12]. A robot is mainly able to determine its position in several ways using internal sensors that directly measure  $q_1$  and  $q_2$  angles of the joints. Hence, we need to show A and B positions in terms of these joints angles. This leads to forward kinematics. Inverse kinematics finds the values of robot joint variables by determining the end-effector position and rotational state. The  $O_0x_0y_0$  base coordinate system is considered in

accordance with figure (2). The  $(x, y)$  system tool coordinates are represented as follow:

$$x = l_1 \cos q_1 + l_2 \cos(q_1 + q_2) \quad (1)$$

$$y = l_1 \sin q_1 + l_2 \sin(q_1 + q_2) \quad (2)$$

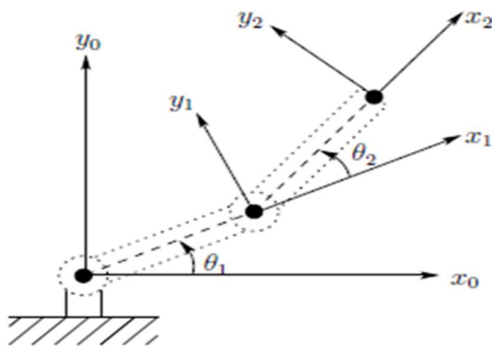


Fig. 2. Two-link planar robot [12]

In which  $l_1$  and  $l_2$  are the lengths of two links. Also the rotational state of the tool coordinate system in relation to the base coordinate system is presented  $y_0$  by the cosines of  $x_2$  and  $y_1$  axes in relation to  $x_0$  and axes with the following relations:

$$\begin{aligned} x_2 \cdot x_0 &= \cos(q_1 + q_2); & y_2 \cdot x_0 &= -\sin(q_1 + q_2) \\ x_2 \cdot y_0 &= \sin(q_1 + q_2); & y_2 \cdot y_0 &= \cos(q_1 + q_2) \end{aligned} \quad (3)$$

The above relations can be combined into a rotation matrix:

$$\begin{bmatrix} x_2 \cdot x_0 & y_2 \cdot x_0 \\ x_2 \cdot y_0 & y_2 \cdot y_0 \end{bmatrix} = \begin{bmatrix} \cos(q_1 + q_2) & -\sin(q_1 + q_2) \\ \sin(q_1 + q_2) & \cos(q_1 + q_2) \end{bmatrix} \quad (4)$$

### 2.2. Dynamic equations of two-link robot arm with Lagrange-Euler method

Dynamic equations explicitly express the relations between force and motion. As shown in figure (2),  $q_1$  and  $q_2$  are the joints angles and  $m_1$  and  $m_2$  are the link mass.

The equations for link (2) will be:

$$x_2 = l_1 \cos q_1 + l_2 \cos(q_1 + q_2) \quad (5)$$

$$y_2 = l_1 \sin q_1 + l_2 \sin(q_1 + q_2) \quad (6)$$

$$\dot{x}_2 = -l_1 \dot{q}_1 \sin q_1 - l_2 (\dot{q}_1 + \dot{q}_2) \sin(q_1 + q_2) \quad (7)$$

$$\dot{y}_2 = l_1 \dot{q}_1 \cos q_1 + l_2 (\dot{q}_1 + \dot{q}_2) \cos(q_1 + q_2) \quad (8)$$

And the Lagrange motion equation is as below:

$$\frac{d}{dt} \frac{\partial L}{\partial \dot{q}} - \frac{\partial L}{\partial q} = \tau \quad (9)$$

Finally, arm dynamic equations will be obtained by nonlinear differential equations based on Lagrange equation.

$$\begin{aligned} \tau_1 &= [(m_1 + m_2)l_1^2 + m_2 l_2^2 + 2m_2 l_1 l_2 \cos q_2] \ddot{q}_1 \\ &+ [m_2 l_2^2 + m_2 l_1 l_2 \cos q_2] \ddot{q}_2 - m_2 l_1 l_2 (2\dot{q}_1 \dot{q}_2 + \dot{q}_2^2) \sin q_2 \\ &+ (m_1 + m_2) g l_1 \cos q_1 + m_2 g l_2 \cos(q_1 + q_2) \end{aligned} \quad (10)$$

$$\begin{aligned} \tau_2 &= [m_2 l_2^2 + m_2 l_1 l_2 \cos q_2] \ddot{q}_1 + m_2 l_2^2 \ddot{q}_2 + m_2 l_1 l_2 \dot{q}_1^2 \sin q_2 \\ &+ m_2 g l_2 \cos(q_1 + q_2) \end{aligned} \quad (11)$$

In summary, the standard form of the planar elbow arm is as follows:

$$M(q)\ddot{q} + C(q, \dot{q}) + G(q) = \tau \quad (12)$$

That  $M(q)$  is the inertial matrix,  $C(q, \dot{q})$  is the matrix including the parts related to the Coriolis and centripetal forces,  $G(q)$  is the gravity torque

vector and  $\tau = \begin{pmatrix} \tau_1 \\ \tau_2 \end{pmatrix}$  is the torque.

$$|q_1| \leq k_{c1}, |q_2| \leq k_{c2}, |\dot{q}_1| \leq k_{c3}, |\dot{q}_2| \leq k_{c4}$$

Indicates the constraints on the arms' angle output and their angular derivative. The expanded relation of (2-12) is represented as follows:

$$\begin{bmatrix} \tau_1 \\ \tau_2 \end{bmatrix} = M(q) \begin{bmatrix} \ddot{q}_1 \\ \ddot{q}_2 \end{bmatrix} + \begin{bmatrix} -m_2 l_1 l_2 (2\dot{q}_1 \dot{q}_2 + \dot{q}_2^2) \sin q_2 \\ m_2 l_1 l_2 \dot{q}_1^2 \sin q_2 \end{bmatrix} + \begin{bmatrix} (m_1 + m_2) g l_1 \cos q_1 + m_2 g l_2 \cos(q_1 + q_2) \\ m_2 g l_2 \cos(q_1 + q_2) \end{bmatrix} \quad (13)$$

That

$$M(q) = \begin{bmatrix} (m_1 + m_2)l_1^2 + m_2 l_2^2 + 2m_2 l_1 l_2 \cos q_2 & m_2 l_2^2 + m_2 l_1 l_2 \cos q_2 \\ m_2 l_2^2 + m_2 l_1 l_2 \cos q_2 & m_2 l_2^2 \end{bmatrix} \quad (14)$$

herefore, the equations governing the two-degree-of- freedom arm are obtained to implement it in simulation [13,14].

### 2.3. The analysis of robot dynamic equations

We need to know the amount of torque required for each joint to achieve the desired motion in order to control robot motion. In Robotics, this approach is called forward dynamics. There have been different challenges to solve robot forward dynamics due to the differential operators. The methods such as the numerical solution of equations in the main Matlab environment, the use of blocks in Simulink, 13 embedded function and the use of mechanical simulation toolkit can be applied that have particular advantages and disadvantages of their own.

### 2.3.1. Using s-function

In this method, the user first writes his dynamic equations in an m-file environment. In this case all state variables and also inputs are introduced to the function. We need a software mediator to introduce this function into the Simulink environment. In this case a function called S-Function is introduced. Although the original code of this s-function has many complications, we can match the dynamic problem with it by an appropriate approach. Thus in this paper s-function method has been used due to its advantages.

### 2.4. The proposed method to control the two-axis robotic arm

The application of neural networks as a powerful tool to approximate functions and fuzzy logic due to system uncertainties and indeterminacies has

been greatly considered by the researchers. Therefore, in this paper a combination of neural and fuzzy networks will be used in both output tracking and approximation of uncertainties in order to control two-axis robotic arm. The neural network used in the adaptive neuro-fuzzy inference system proposed in this article, is a multilayer perceptron neural network with an error back propagation algorithm and the fuzzy method chosen is a Takagi-Sugeno fuzzy inference system.

## 3. Implementation

Robot arm is defined as a kinematic chain of rigid links and each degree of its freedom is controlled by an independent torque. The mathematical model used in the simulation is an elbow robot arm shown in fig.3.

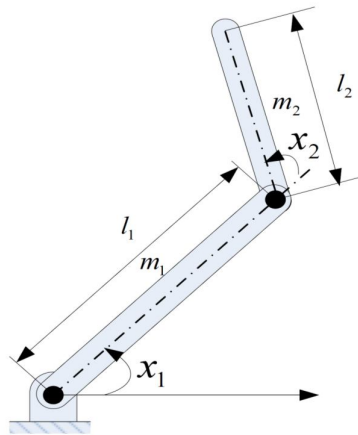


Fig. 3. An elbow robot arm used in the simulation

### 3.1. Two-degree-of-freedom robot

For simulation, the fuzzy system has been used in two parts. In the first part, a fuzzy system is used for the approximation of uncertainties and in the second part an adaptive neuro-fuzzy controller is used replacing  $\text{sgn}(s)$  nonlinear function term to produce appropriate  $k$ s along with proper output tracking.

### 3.2. Implementation of fuzzy part

The implementation details of two fuzzy parts are discussed in the following. First, the adaptive neuro-fuzzy controller will be described as a replacement for switching function in control and then the structure of the fuzzy model replacing the robot arm uncertainties will be examined.

#### 3.2.1. The adaptive neuro-fuzzy controller replacing the switching function

Membership functions related to the input and output are shown in fig.4.

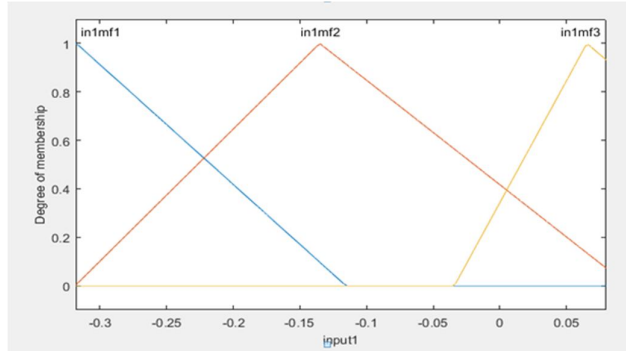


Fig. 4. Membership functions related to the input and output

**3.3. The input membership functions of the takagi-sugeno fuzzy controller**

The number of output membership functions of Takagi-Sugeno fuzzy controller is three and of

linear type. The intended parameters for each of P, Z, and N membership functions are specified below.

Tab. 1. The output membership functions of takagi-sugeno fuzzy controller

Membership function	Output
P=[0.0790 10.76]	output= (0.07902)×input+(10.76)
Z=[-2.279 0.3734]	output= (-2.279)×input+(0.3734)
N=[ -2.742 -0.2563]	output= (-2.742)×input-(0.2563)

The fuzzy system designed is presented in the following table according to fuzzy rules that is in fact the implementation of  $K_i = \text{sgn}(s_i)$  function. The Takagi-Sugeno fuzzy if-then rules can also be represented as follows:

- rule1 : if input1 is mf1 then output is N
- rule2 : if input1 is mf2 then output is Z
- rule3 : if input1 is mf3 then output is P

Thus a part of the robot control law that has an undesirable perturbation behavior is replaced and implemented using the adaptive neuro-fuzzy network structure and the membership functions associated with each of the uncertainty terms are

shown in the following table based on the above formulas.

NB, NS, ZO, PS, PB specifically show the range of different membership functions of  $\ddot{q}_j, \dot{q}_j, q_j$  used, denoting negative big, negative small, zero, positive small and positive big respectively. The results of this section are presented in Fig.5. The approximation of uncertainties fuzzy model is shown by replacing the uncertainty terms with the fuzzy part. As shown in this figure, the uncertainty term of robot arm dynamic model is approximated with an acceptable accuracy by the simulated fuzzy model based on the proposed algorithm.

Tab. 2. The membership functions required for fuzzy approximation

Number	Membership function
1	$\mu_{\dot{q}_j, NB} = \frac{1}{1 + [\exp((\dot{q}_j + 1.13)/0.2)]^2}$ $\mu_{\dot{q}_j, NS} = \exp(-((\dot{q}_j + 0.75)/0.45)^2)$ $\mu_{\dot{q}_j, ZO} = \exp(-(\dot{q}_j/0.45)^2)$ $\mu_{\dot{q}_j, PS} = \exp(-((\dot{q}_j - 0.75)/0.45)^2)$ $\mu_{\dot{q}_j, PB} = \frac{1}{1 + [\exp(-(\dot{q}_j - 1.13)/0.2)]^2}$

$$\begin{aligned}
 2 \quad & \mu_{\ddot{q}_j NB} = \frac{1}{1 + [\exp((\ddot{q}_j + 60)/20)]^2} \\
 & \mu_{\ddot{q}_j NS} = \exp(-((\ddot{q}_j + 40)/30)^2) \\
 & \mu_{\ddot{q}_j ZO} = \exp(-(\ddot{q}_j/30)^2) \\
 & \mu_{\ddot{q}_j PS} = \exp(-((\ddot{q}_j - 40)/30)^2) \\
 3 \quad & \mu_{\ddot{q}_j PB} = \frac{1}{1 + [\exp(-(\ddot{q}_j - 60)/20)]^2} \\
 & \mu_{\dot{q}_j NB} = \frac{1}{1 + [\exp((\dot{q}_j + 0.75)/0.1)]^2} \\
 & \mu_{\dot{q}_j NS} = \exp(-((\dot{q}_j + 0.5)/0.3)^2) \\
 & \mu_{\dot{q}_j ZO} = \exp(-(\dot{q}_j/0.3)^2) \\
 & \mu_{\dot{q}_j PS} = \exp(-((\dot{q}_j - 0.5)/0.3)^2) \\
 & \mu_{\dot{q}_j PB} = \frac{1}{1 + [\exp(-(\dot{q}_j - 0.75)/0.1)]^2} \\
 4 \quad & \mu_{\ddot{q}_{rj} NB} = \frac{1}{1 + [\exp((\ddot{q}_{rj} + 7)/1.5)]^2} \\
 & \mu_{\ddot{q}_{rj} NS} = \exp(-((\ddot{q}_{rj} + 5)/5)^2) \\
 & \mu_{\ddot{q}_{rj} ZO} = \exp(-(\ddot{q}_{rj}/5)^2) \\
 & \mu_{\ddot{q}_{rj} PS} = \exp(-((\ddot{q}_{rj} - 5)/5)^2) \\
 & \mu_{\ddot{q}_{rj} PB} = \frac{1}{1 + [\exp(-(\ddot{q}_{rj} - 7)/1.5)]^2}
 \end{aligned}$$

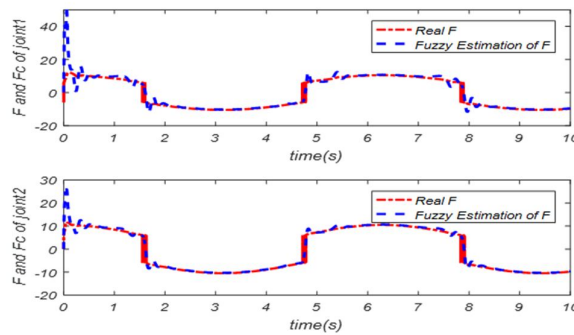


Fig. 5. The comparison of the fuzzy model replacing the uncertainties and the actual amount of uncertainty of the dynamic model

### 3.4. The proposed control law for the two-degree-of-freedom robot arm

The equations governing this robot arm is defined as relation 15 by defining two state variables of two joints 15 by defining two state variables of two joints angular equations using Lagrangian equations:

$$\begin{cases} x_1 = \theta_1 = q_1 \\ x_2 = \theta_2 = q_2 \end{cases}$$

$$D(q)\ddot{q} + C(q, \dot{q})\dot{q} + G(q) + F_r(\dot{q}) + \tau_d = \tau \quad (15)$$

Where  $q \in R^n$  is the arm angular position,  $D(q) \in R^{n \times n}$  is the symmetric and constrained positive definite inertia matrix,  $C(q, \dot{q})\dot{q} \in R^n$  shows the central and Coriolis torques, and

$F_r(\dot{q}) \in R^n$ ,  $G(q) \in R^n$ ,  $\tau \in R^n$  and  $\tau_d \in R^n$  represent the gravity torques, friction, turbulences and the torque applied to the joint respectively.

Also,  $m_2, m_1$  shows the mass of arms and  $l_2, l_1$  is their length. The robot arm uncertainties can be written as:

$$D(q)\ddot{q} + C(q, \dot{q})\dot{q} + G(q) + F(q, \dot{q}, \ddot{q}, t) = \tau \quad (16)$$

Where  $F(q, \dot{q}, \ddot{q}, t)$  shows friction, turbulence and load change and  $D, C, G$  include the load carrying capacity parameter. In the (16)  $D(q)$ ,  $C(q, \dot{q})\dot{q}$ ,  $G(q)$  are definite and all the state variables are available for measurement.  $F(q, \dot{q}, \ddot{q}, t)$  is a completely unknown nonlinear

function vector that should be replaced with a multi-input-multi-output fuzzy system. Thus the following control law can be formulated.

$$\tau = D(q)\ddot{q}_r + C(q, \dot{q})\dot{q}_r + G(q) + \hat{F}(q, \dot{q}, \ddot{q}|\Theta) - K_D s - W \text{sgn}(s) \tag{17}$$

Where  $K_D = \text{diag}(K_i)$ ,  $K_i > 0, i = 1, 2, \dots, n$  and  $W = \text{diag}(w_{M_1}, \dots, w_{M_n})$ , thus in the following, the adaptive neuro-fuzzy controller is implemented based on the above relation control law.

### 3.5. The simulation results of the proposed controller based on the adaptive neuro-fuzzy network

As the Simulink model of the proposed controller is shown in fig.6, the system under study is composed of the adaptive hybrid neuro-fuzzy controller and function approximation fuzzy model.

In the following, the above system will be simulated and its ability to track the angular reference input and angular velocity within a specified range (complete constraint) will be shown.

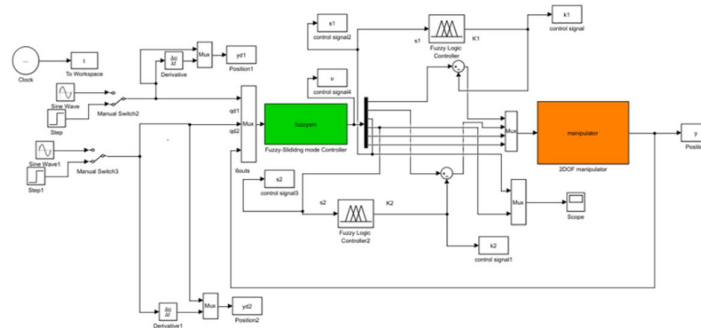


Fig. 6. The Simulink model of the proposed adaptive neuro-fuzzy controller

#### 3.5.1. Sine reference input tracking

The proposed controller function is evaluated in this section. For the sine reference input and the constraint on the angular range of arms,

$|\theta_1| \leq 0.3, |\theta_2| \leq 0.3$  the output response of the ideal angles of robot arm joints using the proposed controller, is shown in fig.7.

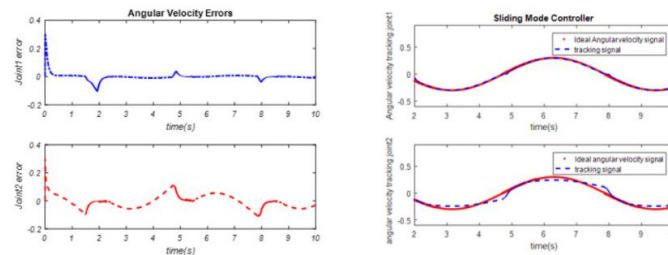
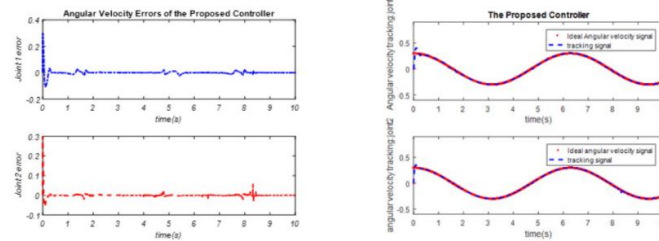


Fig. 7. Robot arm joints angular tracking according to sine reference input and the amount of robot arm joints angular error in the proposed controller

Fig. 7 shows the error associated with each of the robot arm joints. As it is clear in this figure, the proposed controller has been able to accurately track the ideal sine output and angular error is negligible.

Moreover, for the sine reference input derivative and the constraint on the range of arm angular velocity,  $|\dot{\theta}_1| \leq 0.3, |\dot{\theta}_2| \leq 0.3$  the output response of the ideal angles of robot arm joints using the proposed controller is shown in Fig.8.



**Fig. 8. Tracking of the constrained angular velocity of robot arm joints according to the sine reference input and the amount of angular velocity error of robot arm joints**

The angular velocities of two robot joints are limited to the range of  $|\dot{\theta}_1| \leq 0.3, |\dot{\theta}_2| \leq 0.3$ . As shown in Fig.8 according to the negligible error seen in the robot arm angular velocities the proposed controller has been able to track the ideal angular velocities with a desirable accuracy.

The requested control signal for sine input tracking is shown in Fig.9. As it is clear, the amplitude of control signal effort is acceptable. Therefore, it is practically possible to apply these signals.

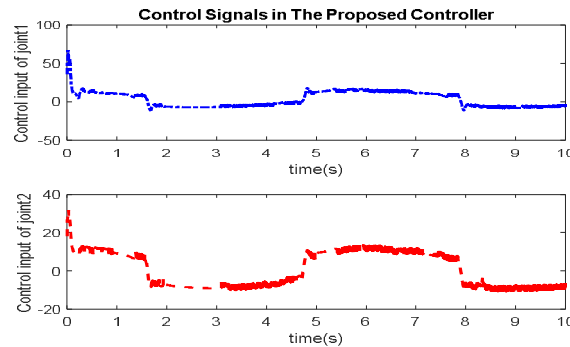


**Fig. 9. The requested control signals according to sine input tracking**

### 3.5.2. Single step reference input tracking

In this section the proposed controller function has been evaluated. For the step reference input

shown in Fig.10 the output response of the ideal angles of robot arm joints is represented using the proposed controller.

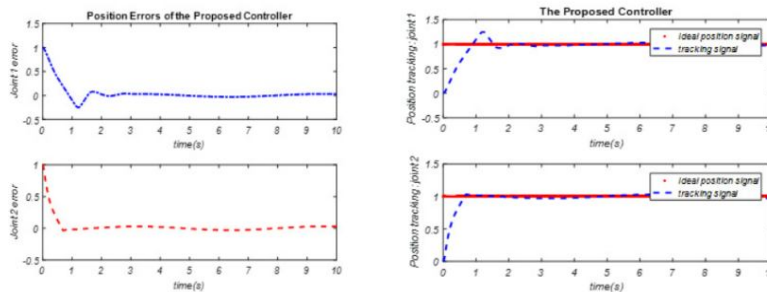


**Fig. 10. Robot arm joints angular tracking according to step reference input and the amount of angular error of the proposed controller robot arm joints**

Fig.10 shows the error related to each of the robot arm joints. As it is clear in this figure, except for the initial moments, the controller has been able to track the ideal output of the single step input with the desired accuracy and negligible error. Fig.11 shows the single step angular velocity

tracking and the error associated with each of robot arm joints. As it is represented in this figure, the proposed controller except for the initial moments has been able to track the sine ideal output and its angular velocity error is negligible.



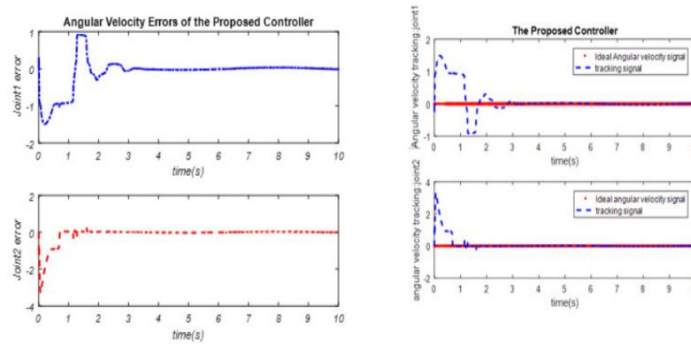


**Fig. 11. The constrained angular velocity tracking of the proposed robot controller arm joints and the constrained angular velocity error of robot arm joints according to the derivative of single step reference input**

As the simulation results show in these figures, the proposed adaptive neuro-fuzzy controller has been able to successfully track the single step reference input. Therefore, the proposed controller has the ability to track the standard sine and single step inputs with an acceptable accuracy.

**3.6. The study on the length changes of the robot arm**

In this section, we examine the effect of length changes of the robot arm. As shown in the previous wave forms, we have the best track and response for the arm length of  $L1=1m$  and  $L2=0.8m$  compared to the Ville sine inputs. However, as shown in figures 12 and 13, the input signal tracking is not done well with  $L1=1.7m$  and  $L2=0.5m$  length changes of the robot arm and we will see the unwanted fluctuations in the control signal applied to the robot links.

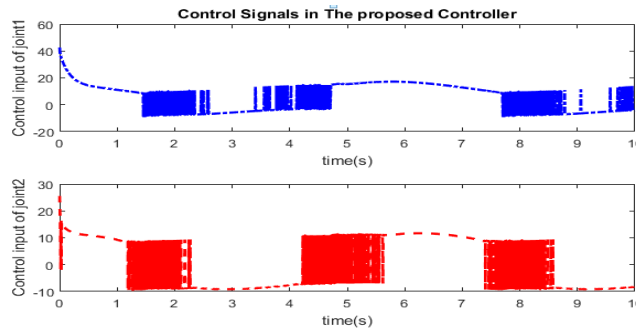


**Fig. 12. The unwanted fluctuations in the control signal with the length changes of the robot arm**

However, along with these changes, we will see again the unwanted fluctuations in the control

signal applied to the robot joints with the length changes of the robot arms,  $L1=2m$  and  $L2=1.5m$ .

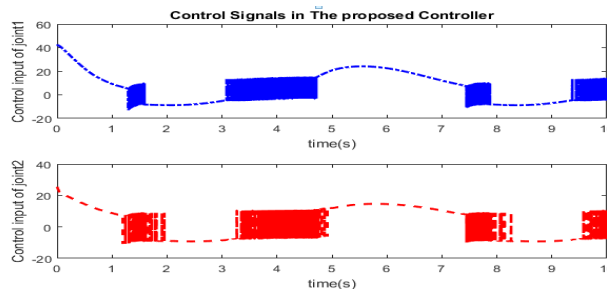


**Fig. 13. The unwanted fluctuations in the control signal with the length changes of the robot arm**

### 3.7. The comparison of the proposed controller with the nonlinear sliding mode controller

In this section, we compare the proposed controller with the sliding mode controller that is a classic nonlinear controller frequently used in the robot control. Thus the output of the angles

position and the control signal required for tracking are examined. As shown in Fig.14, the proposed controller has better performance in output tracking. Also, the control signal in the proposed method has fewer fluctuations than the classic sliding mode method.

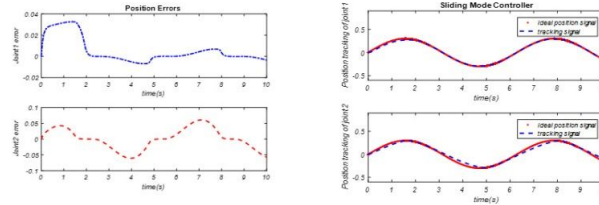


**Fig. 14. The sine angular tracking of robot arm joints in the classic sliding mode controller and the amount of the angular error of robot arm joints in the sliding mode controller**

The angular error of the robot arm joints in the sliding mode controller is shown in Fig.15 that is obtained by the difference between the ideal signal and the tracking signal. The angular velocity response of the robot arm joints and the angular velocity error for the sine reference input derivative in the classic sliding mode controller is shown in Fig.16. The results indicate a significant error in the angular velocity tracking.

Thus it is obvious that the proposed controller has noticeable advantages for the sine input compared to the sliding mode controller. In the following we will study the simulation results of the sliding mode controller for the single step input. Fig.15 shows the angular velocity tracking of the single step reference input and the error related to each of the robot arm joints. As it is evident in this figure, the sliding mode controller has slight steady-state error.

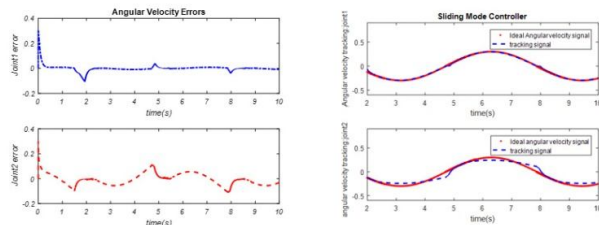


**Fig. 15. The sine tracking of the angular velocity of the robot arm joints in the classic sliding mode controller and the amount of the angular velocity error of the robot arm joints**

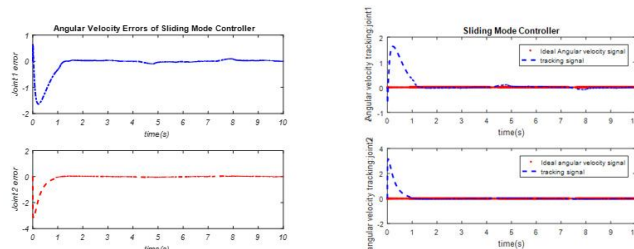


**Fig. 16. The constrained angular velocity tracking of the sliding mode controller robot arm joints and the constrained angular velocity error of the robot arm joints in the sliding mode controller**

However, as it is clear in this method, the control signal has chattering fluctuations in tracking the

single step input shown in fig. 17 that practically makes it impossible to use this controller alone.

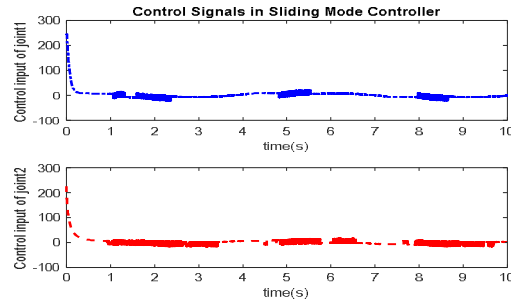


Fig. 17. The control signals of the robot arm joints in the classic sliding mode controller

The results of the comparison of two simulation methods for the angular error and angular

velocity of the robot arm joints can be summarized in tables 3 to 6.

**Tab. 3. The angular error of two robot joints (sine input)**

The angular error of two robot joints (sine input)	First method	Second method
Controller type	Sliding mode	Adaptive neuro-fuzzy network
Root mean square error (RMSE) (angle $\theta_1$ )	0.000012	0.000011
Root mean square error (RMSE) (angle $\theta_2$ )	0.0047	0.0045

**Tab. 4. The angular velocity error of two robot joints (sine input)**

The angular velocity error of two robot joints(sine input)	First method	Second method
Controller type	Sliding mode	Adaptive neuro-fuzzy network
Root mean square error (RMSE) (angle $\theta_1$ )	0.0064	0.0060
Root mean square error (RMSE) (angle $\theta_2$ )	0.0064	0.0060

**Tab. 5. The angular error of two robot joints (single step input)**

The angular error of two robot joints (single step input)	First method	Second method
Controller type	Sliding mode	Adaptive neuro-fuzzy network
Root mean square error (RMSE) (angle $\theta_1$ )	0.0058	0.0057
Root mean square error (RMSE) (angle $\theta_2$ )	0.0058	0.0057

**Tab. 6. The angular velocity error of two robot joints (single step input)**

The angular velocity error of two robot joints(single step input)	First method	Second method
Controller type	Sliding mode	Adaptive neuro-fuzzy network
Root mean square error (RMSE) (angle $\theta_1$ )	0.0064	0.0060
Root mean square error (RMSE) (angle $\theta_2$ )	0.0064	0.0060

According to it we can generally conclude that by comparing the sliding mode and proposed adaptive hybrid neuro-fuzzy controller, the proposed controller for both sine and single step input has had relatively better response and higher accuracy in the reference input tracking compared to the proposed classic controller but their significant difference is reflected in the chattering in their control signals, in a way that the proposed method in particular has better capability to remove the chattering of control signals applied to the robot operators.

#### 4. Conclusion

In this paper the adaptive hybrid neuro-fuzzy control method on a two-degree- of freedom robot arm was examined. In fact, the proposed method is a combination of Takagi-Sugeno fuzzy controller and the training algorithm of multilayer neural networks that the tracking direction of their angles and velocity is used. The fuzzy system is used in two parts of the simulation of this thesis. In the first part, a fuzzy system is used for the approximation of the uncertainties of robot arm dynamic model in the control law and in the second part an adaptive neuro-fuzzy controller is applied to replace the function nonlinear term for proper production along with appropriate input tracking.

Infact the switching function in the control law is replaced by an adaptive neuro-fuzzy network. The simulation results showed that the proposed controller has been able to track the ideal sine input with the desired accuracy for each of the robot arm joints except in the early moments and its angular velocity error under the specified constraints is negligible. The final control system has ideal characteristics in tracking the angles of two joints and the angular velocity within the permitted range and its control signal can be applied, in practice, to the system stimulators. The chattering phenomenon that has undesirable effect on the operators in the closed loop system is favorably weakened in this design.

Then, we evaluated the sine reference and single step input tracking. The observations show that the proposed controller according to the sine reference and single step input tracking has more accuracy than the classic methods such as the sliding mode. The comparison of the simulation results with the classic sliding mode controller suggests more ideal performance of the intelligent method based on the proposed adaptive neuro-fuzzy controller in reference signal tracking with slight tracking error and reduced chattering in the control signal along with the improved maximum overshoot and settling time.

As seen in this study, the proposed adaptive neuro-fuzzy control can be used for the reference input tracking with a desired accuracy. However, to improve the controller, the effect of membership functions on improving the reference input tracking and also more reducing the chattering phenomenon in the control signals applied to the robot arm can be examined or the feedback dynamic neural network model can be used as a replacement for the Takagi-Sugeno fuzzy model.

#### References

- [1] Sayenko D. G. Nguyen R. Hirabayashi T. Popovic M. R. Masani K. Method to Reduce Muscle Fatigue During Transcutaneous Neuromuscular Electrical Stimulation in Major Knee and Ankle Muscle Groups. *Neurorehabilitation and neural repair*. (2014).
- [2] Klamka J. Controllability of dynamical systems. A survey. *Bulletin of the Polish Academy of Sciences: Technical Sciences*. Vol. 61, No. 2, (2013), pp. 335-342.
- [3] Mustapha M., Amir A. B. Umar Z. Salinda B. Anita A. Mohamad A. Sh. Velocity control of a two-wheeled inverted pendulum mobile robot: a fuzzy model-based

- approach. *Bulletin of Electrical Engineering and Informatics*. Vol. 8, No. 3, (2019), pp. 808-817.
- [4] Wahyu S. P. Enggar A. Andy R. Dian P. H. Simulation design of trajectory planning robot manipulator. *Bulletin of Electrical Engineering and Informatics*, Vol. 8, No. 1, (2019), pp. 196-205.
- [5] Sevil A. Petrov M. Trajectory Control of Mobile Robots using Type-2 Fuzzy-Neural PID Controller. *Elsevier IFAC*. (2015), pp. 138-143.
- [6] Sandy A. D. Handayani T. Darlis H. Robot Motion Control Using the Emotiv EPOC EEG System. *Bulletin of Electrical Engineering and Informatics*. Vol. 7, No. 2, (2018), pp. 279-285.
- [7] Xu B., Ch. Yang and Zh. Shi. Reinforcement Learning Output Feedback NN Control Using Deterministic Learning Technique.” *IEEE Transactions on Neural networks and learning systems*, Vol. 25, No. 3, (2014).
- [8] Ahmad S. Zhang H. Liu G. Distributed fault detection for modular and reconfigurable robots with joint torque sensing: A prediction error based approach. *Elsevier, Mechatronics*. Vol. 23, (2013), pp. 607- 616.
- [9] T. Y. Aji A. F. Eva I. A. Robotic Leg Design to Analysis the Human Leg Swing from Motion Capture. *Bulletin of Electrical Engineering and Informatics*. Vol. 6, No. 3, (2017), pp. 256-264.
- [10] Philip Chen C. L. Wen G. Liu Y. Wang F. Adaptive Consensus Control for a Class of Nonlinear Multiagent Time-Delay Systems Using Neural Networks. *IEEE Transactions on Neural networks and learning systems*. Vol. 25, No. 6, (2014).
- [11] Philip Chen C. L. Liu Y. Wen G. Fuzzy Neural Network-Based Adaptive Control for a Class of Uncertain Nonlinear Stochastic Systems. *IEEE Transactions on Cybernetics*. Vol. 44, No. 5, (2014).
- [12] Mark W. Seth Hutchinson S. Vidyasagar M. Robot Modeling and Control. *JOHN WILEY & SONS, INC*. (2005). First Edition.
- [13] Er M. J. Sun Y. L. Hybrid fuzzy proportional-integral plus conventional derivative control of linear and nonlinear systems. *IEEE Transaction on Industrial Electronics*. Vol. 48, No. 6, (2001), pp. 1109-1117.
- [14] Song Z. Yi J. Zhao D. Li X. A computed torque controller for uncertain robotic manipulator systems: fuzzy approach. *Fuzzy Sets and Systems*. Vol. 154, (2005), pp. 208-226.

Follow This Article at The Following Site:

Dehyadegari L, Khajehasani S. Robot Control by Using Intelligent Systems Considering Complete Constraints. *IJIEPR*. 2021; 32 (1) :79-91  
URL: <http://ijiepr.iust.ac.ir/article-1-1086-en.html>

